JCTC Journal of Chemical Theory and Computation

Transition-State Theory, Dynamics, and Narrow Time Scale Separation in the Rate-Promoting Vibrations Model of Enzyme Catalysis

Baron Peters

Departments of Chemical Engineering and Chemistry and Biochemistry, University of California, Santa Barbara, California 93106

Received January 26, 2010

Abstract: The power of transition-state theory (TST) for understanding enzymes is evidenced by its recent use in the design and synthesis of highly active de novo enzymes. However, dynamics can influence reaction kinetics, and some studies of rate-promoting vibrations even claim that dynamical theories instead of TST are needed to understand enzymatic reaction mechanisms. For the rate-promoting vibration (RPV) model of enzyme catalysis [Antoniou et al., *J. Chem. Phys.* **2004**, *121*, 6442], a reactive flux correlation function analysis shows that dynamical effects do slow the kinetics. However, the RPV model also shows extremely long-lived correlations because the RPV and the bath are not directly coupled. Additionally, earlier studies of the RPV model show a narrow time scale separation due to a small 5kT barrier. Thus earlier findings based on the RPV model may have little bearing on the properties of real enzymes. The intrinsic reaction coordinate (IRC) reveals that the RPV is an important component of the reaction coordinate at early and late stages of the pathway, but the RPV is not an important component of the reaction coordinate direction at the transition state. The unstable eigenmode from harmonic TST (which coincides with the IRC at the saddle point) gives a larger transmission coefficient than the coordinate used in the correlation functions of Antoniou et al. Thus while TST cannot predict the transmission coefficient, the RPV model suggests that TST can provide mechanistic insights on elementary steps in enzyme catalysis. Finally, we propose a method for using the transition-state ensemble as predicted from harmonic TST to distinguish promoting vibrations from other more mundane bath variables.

Introduction

Enzymes are remarkably active and selective catalysts.[1–3] Their catalytic activity at room temperature and mild pH provide exciting alternatives to processes using comparatively harsh conditions.[4] Because enzymes catalyze elementary reactions that break and make bonds much stronger than kT, many investigators use harmonic transition-state theory (TST),[5–8] variational TST,[9,10] and related theories[11–14] to analyze enzymatic catalysis mechanisms. These theories quantify how the enzyme enhances the rate by lowering an activation barrier through electrostatic,[15,16] covalent,[17] or other factors[18–21] that influence the thermodynamics. Mixed quantum mechanics/molecular mechanics (QM/MM)[14,15,22,23] calculations and empirical valence bond (EVB) models[24] are frequently combined with TST to understand these important aspects of enzymatic reaction mechanisms. Tunneling is also important for enzymatic reactions that involve proton or hydrogen transfer.[7,21,25–30] These methods and theories show extraordinary predictive abilities.[31,32] For a striking example, these approaches have recently been used to create highly active *de novo* enzymes.[33,34]

For some activated processes, dynamical effects are also important.[35–41] For many bond-making and -breaking reactions, these effects can be treated as secondary corrections to the TST rate.[32,42–44] However, some recent computational studies note problems with TST[45] and suggest that dynamical theories are essential for understanding enzymatic reaction mechanisms.[46–49] Of particular interest in this work is the

10.1021/ct100051a
Published on Web 04/09/2010

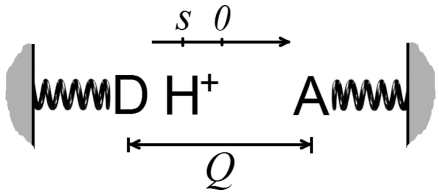

Figure 1. Mechanical model of the rate-promoting vibrations in enzymatic proton transfer reactions. The barrier for proton transfer depends on the donor (D) and acceptor (A) distance.

rate-promoting vibrations (RPV) model of enzyme catalysis.[46] This paper highlights some surprising new findings on dynamics of barrier crossing in the RPV model. We find that parameters used in previous implementations[46] give only a narrow time scale separation and long-lived correlations in the dynamics of the rate-promoting mode. We provide evidence that a lack of direct coupling between the bath and the rate-promoting mode can lead to energy diffusion limitations[5] that may not resemble dynamics in real enzymes. We also compare the unstable eigenmode coordinate from harmonic TST to the reaction coordinates investigated by Antoniou and Schwartz. Our results confirm that TST can be used to understand enzymatic reaction mechanisms that involve promoting vibrations, but perhaps not to the extent which dynamical effects will reduce the rate constant. We conclude by suggesting a simple procedure to identify promoting variables using only the information that is available from a TST analysis.

Dynamics in the Rate-Promoting Vibrations Model

The rate-promoting vibrations (RPV) model of enzyme catalysis[21,46] includes two key variables, s and Q. Q represents donor−acceptor distance, and s corresponds to the position of a proton along the path between donor and acceptor. Figure 1 depicts a mechanical model of the donor and acceptor atoms in the RPV model. The model potential as a function of s and Q includes a quartic bistable barrier of height V_0, a harmonic "promoting vibration" coordinate Q with frequency ω_Q, a term that couples s and Q, and a bilinear coupling between s and bath modes $\boldsymbol{q}$:

$$V = V_0(1 + s^4 - 2s^2) + c(s^2 - 1)Q + \frac{1}{2}m_Q\omega_Q^2Q^2 + \frac{1}{2}\sum_{k=1} m_k\omega_k^2\left(\boldsymbol{q}_k - \frac{c_k s}{m_k\omega_k^2}\right)^2 \quad (1)$$

The harmonic bath has a Debye frequency distribution.[46] The minima of V are at $(s, Q) = (\pm 1, 0)$ regardless of ω_Q, but the saddle point $(s^*, Q^*) = (0, c/m_Q\omega_Q{}^2)$ shifts to higher Q values as ω_Q decreases.

Antoniou et al.[46] used transition-path sampling (TPS)[50−52] to study the RPV model. Their path ensemble includes only those 4 ps trajectories that spend the first 1 ps and last 2 ps entirely within the reactant and product basins, respectively.[46] Antoniou et al. report a dynamical rate-promoting effect that depends nonmonotonically on ω_Q.[46] The parameters used by Antoniou et al. were $V_0 = 6$ kcal/mol, $c = (V_0m_Q\omega_Q{}^2)^{1/2}$,

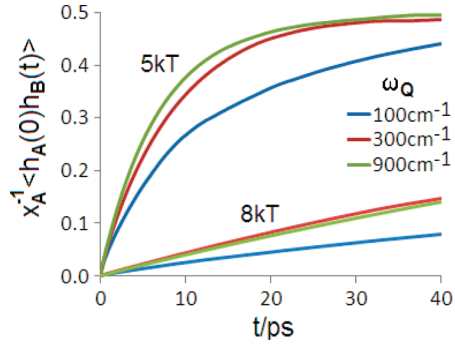

Figure 2. The correlation function $C(t)$ for three values of the rate-promoting vibration frequency at two barrier heights, 5 and 8kT.

$T = 300$ K, $m_Q = 12$ amu, and $m_S = 1$ amu.[46] They investigated promoting vibrational frequencies of $\omega_Q = 100$, 300, and 900 cm^{-1}. Their parameters give a saddle point at $V_0/2$ above the two minima regardless of ω_Q. Their saddle is thus only 5kT above the minima, pushing the limits of the minimal time scale separation that is required for defining a rate constant.[5] Here, we also report new results for the model using a higher 8kT barrier by setting $V_0 = 9.6$ kcal/mol. The masses associated with bath modes were not specified in the original study, but following the convention in later work by Antoniou and Schwartz,[53] we set all bath masses equal to the mass of the promoting vibration. Our analysis of the dynamics is based on the correlation function:[37]

$$C(t) = x_A^{-1} < h_A(0)h_B(t) > \quad (2)$$

where $h_A(t) = 1$ if $s(t) > 0$ and $h_A(t) = 0$, otherwise, $h_B(t) = 1$ if $s(t) < 0$ and $h_B(t) = 0$ otherwise, and $x_A = <h_A(t)>$. For each condition (six total from two barrier heights and three frequencies), we computed the correlation functions from a single 200 ns trajectory. Figure 2 shows the correlation function $C(t)$.

The derivative dC/dt should decay from the TST rate constant to a plateau at the dynamically correct rate constant after a short a molecular relaxation time.[37] The lack of a plateau indicates a narrow or perhaps nonexistent time scale separation.[5] When time scale separation breaks down, the rate constant no longer exists because the waiting time for the next reactive event becomes dependent on the detailed initial condition in phase space. A theoretically motivated model[37,54] for the reactive flux correlation function is

$$\mathrm{d}C/\mathrm{d}t = x_B[(\tau_{TST}^{-1} - \tau_{rxn}^{-1})\exp(-t/\tau_{mol}^{-1}) + \tau_{rxn}^{-1}\exp(-t/\tau_{rxn})] \quad (3)$$

where $\tau_{TST}^{-1} = k_{TST}/x_B$, $\tau_{rxn}^{-1} = k/x_B$, $x_B = 1 - x_A$, k_{TST} is the TST rate constant from states A to B, and τ_{mol} is the (short) time required to commit to a basin from a typical initial condition on the dividing surface between states A and B. Despite the lack of a proper plateau in dC/dt, in some cases $\tau_{rxn}{}^{-1}$ may still be identified from a best fit of dC/dt to the model in eq 3.

Figure 3 shows dC/dt for the 5kT and the 8kT barriers at each of the promoting vibration frequencies. The 8kT barrier

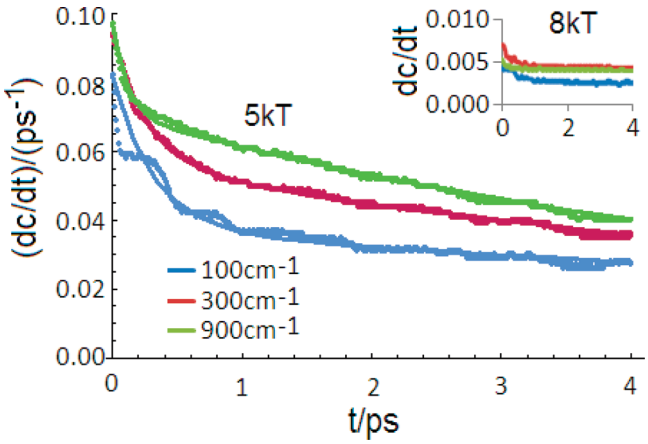

Figure 3. The reactive flux correlation function dC/dt for a barrier of 5kT and of 8kT at each of the three promoting vibrational frequencies. For the 5kT barrier, the time scales are not sufficiently separated to show a clear plateau, so least-squares fits of eq 2 are also shown as smooth curves behind the data. The fit provides an estimate of the reaction and molecular relaxation time scales.

Table 1. Least-Squares Fit Parameters for the Double Exponential Model of the Reactive Flux Correlation Function[a]

ω_Q	τ_{TST}/ps	τ_{RXN}/ps	τ_{MOL}/ps	test
100 cm^{-1}	6.10	13.38	0.314	0.014
300 cm^{-1}	5.32	8.96	0.272	0.010
900 cm^{-1}	5.15	7.10	0.117	0.003

[a] The last column 'test' shows the left-hand side of the inequality (3), which should be much smaller than unity to interpret τ_{rxn} as an inverse rate constant.

gives a clear plateau in dC/dt, but the 5kT barrier does not. However, dC/dt for the 5kT barrier still suggests two time scales: a molecular relaxation time scale shorter than 1 ps and a longer "reaction time scale" that depends strongly on the barrier height. Figure 3 also shows a least-squares fit of the model in eq 3 to the reactive flux correlation function for the 5kT barrier. The reaction time scale is on the order of 100 ps for the 8kT barrier but only about 10 ps for the 5kT barrier. For the 5kT barrier, the molecular relaxation and the reaction time scales are narrowly separated by just over a single order of magnitude. The parameters from a least-squares fit of the correlation function data to eq 3 are given in Table 1.

The fit parameter τ_{rxn}^{-1} will only yield a meaningful rate constant if the flux resulting from the fast molecular relaxation is much less than the flux from the more slowly decaying exponential. Equivalently, for $C(t)$, we require that nearly all of the relaxation from zero to x_B occurs after τ_{mol}. For poor dividing surfaces or small barriers where states near the dividing surface are significantly populated at equilibrium, much of the decay in $C(t)$ may occur during the initial time τ_{mol}. Separately integrating the two flux contributions from the model in eq 3 gives the requirement that

$$\left(\frac{\tau_{mol}}{\tau_{TST}} - \frac{\tau_{mol}}{\tau_{rxn}}\right)x_B << 1 \qquad (4)$$

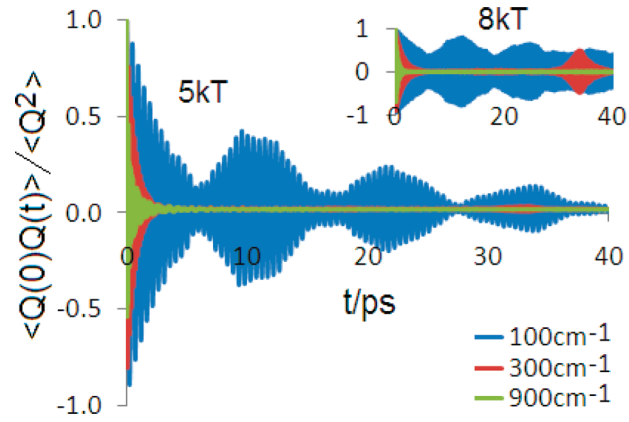

Figure 4. Autocorrelation functions for the rate-promoting vibration $Q(t)$. The inset shows the autocorrelation function when the barrier is 8kT, and the main plot is for a 5kT barrier.

A subtle feature in the correlation functions is the distinctly nonexponential bump around $t = 10$ ps in $C(t)$ for a 100 cm^{-1} promoting vibration and the 5kT barrier. Figure 4 shows the autocorrelation function for the promoting variable $Q(t)$ to help understand the origin of the nonexponential feature. The autocorrelation function reveals long-lived excitations and surprising "beats" in the dynamics of Q.

For both barrier heights at $\omega_Q = 100$ cm^{-1}, the time for the autocorrelation of $Q(t)$ to decay is similar to the time scale for $C(t)$ to relax. This is consistent with the coupling in the RPV model: Q is coupled only to s, and the coupling is strongest when the (s, Q) subsystem has enough potential energy to cross the barrier. To verify this feature of the dynamics, note that the equation for Q:

$$m_Q\ddot{Q} = -m_Q\omega_Q^2 Q - c(s^2 - 1) \qquad (5)$$

can be solved for any initial conditions in Q and for any trajectory $s(t)$:

$$Q(t) = Q_0\cos[\omega_Q t] + \frac{\dot{Q}_0}{\omega_Q}\sin[\omega_Q t] - \frac{c}{m_Q\omega_Q^2}(s^2(t) - 1) + \frac{c}{m_Q\omega_Q^2}\int_0^t \cos[\omega_Q(t - \tau)]2s(\tau)\dot{s}(\tau)d\tau \qquad (6)$$

The solution in eq 6 can give beats when $s(t)$ contains frequencies commensurate with ω_Q. In a real system, Q would be unlikely to show weak coupling artifacts, and thus the RPV model might be improved by directly coupling Q to the bath. In an earlier analysis, Caratzoulas et al.[55] showed how a simple Markovian friction could be added to the dynamics of Q.

Later work by Antoniou and Schwartz[53] used 10 times fewer bath modes with the same individual coupling strengths as in their 2004 study. Again, in the later study, the rate-promoting vibration Q was not directly coupled to a bath. The smaller bath also resulted in significantly weaker coupling to the coordinate s. The section below will show that the coupling in the later study is sufficiently weak that energy diffusion limitations begin to appear.

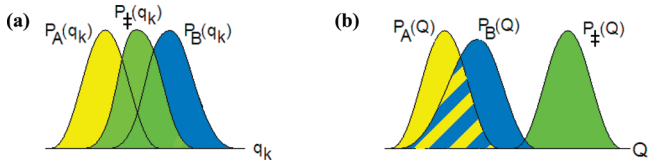

Figure 5. (a) Bath-mode distributions in the transition-state ensemble "interpolate" between the distributions in the reactant and product states. (b) In qualitative contrast, the transition-state ensemble distribution of a promoting variable Q like that of the RPV model does not interpolate between the corresponding reactant and the product distributions. Furthermore, the transition- and stable-state distributions of Q have a small overlap. These characteristics indicate that Q is involved in early and late stages of the reaction coordinate, even when it appears to be uninvolved in the reaction coordinate at the transition state.

Reaction Coordinate

Antoniou and Schwartz[53] performed extensive analyses of possible reaction coordinates for the RPV model. Much of the focus in earlier investigations was to develop strategies to identify special "rate-promoting vibrations" that might participate in the reaction coordinate among more mundane bath variables.[53,55] Two strategies were proposed: one based on the dynamical signature of a rate-promoting vibration in the flux correlation functions[55] and another strategy based on identifying coordinates, whose distributions have a narrow variance in the transition-state ensemble.[53]

The procedure of Caratzoulas et al. is a viable approach for detecting the presence of a rate-promoting vibration, but it does not identify the specific rate-promoting mode.[55] This discussion primarily addresses the later approach of Antoniou and Schwartz. They compute committor probability estimates at points along the harvested transition paths to collect a sample of transition states.[53] They then project that sample onto trial coordinates, e.g., onto s, Q, and various bath modes.[53] Finally, they identify coordinates that give the narrowest projected distribution as coordinates that are important in the reaction coordinate.[53] There are some reasons to suspect this procedure will not work for real systems.

First, it is questionable whether distributions from pairs of coordinates with different units in a real system can be meaningfully compared. Second, Antoniou and Schwartz extensively discuss the *width* of the Q-distribution in the sample of transition states,[53] but it is *the lack of overlap* between the transition-state and equilibrium distributions of Q that most clearly implicates Q in the pre- and reorganization stages. [Antoniou and Schwartz have switched the labels for Figure 1b and c in their paper.][53] Figure 5 provides a schematic example of how overlaps can be used to identify promoting variables that are important at early and late stages of the reaction, but whose involvement may not be clear from the a narrow distribution in the transition-state ensemble.

Third, the strategy of Antoniou and Schwartz finds only the separatrix, i.e., the locus of transition states.[53] Similarly, the approach of Best and Hummer only optimizes the separatrix.[56] However, other strategies discussed in their paper[57–59] optimize the reaction coordinate at all stages of the reaction, including the separatrix.[57–60] An accurate reaction coordinate at all stages[61] is useful for constructing coarse-grained models of the barrier crossing dynamics[62] and for avoiding hysteresis effects[12] that may occur if the reaction coordinate poorly describes early and late stages of the reaction. Figure 6 provides an example of the hysteresis problem from a recent study of methane diffusion in natural gas hydrates.[63]

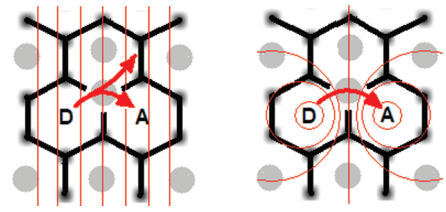

Figure 6. Schematic of methane (gray circles) diffusion by hopping through a water vacancy in a clathrate hydrate (black hexagonal lattice). Left: A calculation of the free energy barrier between donor (D) and acceptor (A) using hyperplane coordinates gave hysteresis because one of the two ways to proceed from the separatrix leads away from the vacant acceptor cage. Right: A bipolar coordinate system *with the same separatrix* gave no hysteresis because it better describes the early and late stages.

Antoniou and Schwartz[53] do not compare the computational cost of their procedure to other approaches. Here, we provide estimates and comparisons to the aimless shooting and likelihood maximization approach using information in their paper.

(1) The footnote in ref 13 of their paper[53] reveals that their implementation of transition-path sampling has an efficiency of less than 1%. The low efficiency results because their implementation of transition-path sampling was not optimized for studying dynamics at sharp saddle-point-type transition states. Aimless shooting can be tuned (by setting $\delta t = 1-2$ fs)[59] to more efficiently sample such sharp barriers.

(2) After computing transition paths, the authors identify 121 transition states by estimating the committor probability at configurations along the paths.[53] Each p_B estimate requires on the order of 100 trajectories.[52,61] Assuming that a small fraction of the points where p_B estimates were computed were found to be transition states, a reasonable estimate for the number of additional trajectories to identify the transition-state ensemble is more than 10 000. Likelihood maximization has been shown to identify a coordinate that is accurate at all stages in model systems[58,62] and in atomistic simulations[64–67] with approximately 1000 trajectories.

(3) Also note that the version of committor analysis used in refs 48 and 43 constrains multiple variables separately. For example, Antoniou and Schwartz[53] applied the two simultaneous constraints $s = 0$ and $Q = c/m_Q\omega_Q^2$. Their version of committor analysis with multiple constraints is less stringent than the usual committor analysis procedure.[52,68,69] Because of the extra constraints, the p_B histogram test does not reflect the accuracy of a true dividing surface through which an observable rate could be computed. We recommend the improved version of committor analysis with the

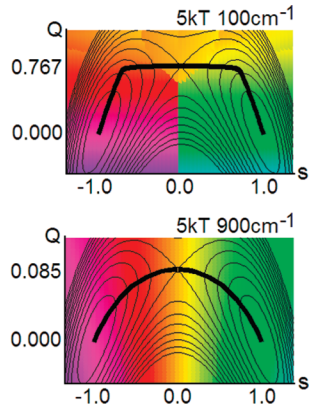

Figure 7. Steepest-descent path (heavy black curve) in mass-weighted coordinates with $m_Q = 12$ and $m_s = 1$ amu (proton). Also shown are contours of $V(s, Q)$ and the scalar arclength coordinate as a color-field background. Results are for $\omega_Q = 100$ cm^{-1} (above) and $\omega_Q = 900$ cm^{-1} (below) with parameters that give a 5kT barrier. Note how ω_Q changes $V(s, Q)$ and the arclength coordinate.

binomial-error deconvolution to isolate reaction coordinate error from committor estimate error.[61]

Aimless shooting and likelihood maximization have some quantitative and qualitative advantages over the approach of Antoniou and Schwartz, but for many enzymatic reactions, an accurate and efficient approach is to identify a saddle point on the energy landscape[70] and then to apply TST.[6] For reactions with sharp barriers that correspond to the breaking and making of chemical bonds, harmonic TST can often provide many mechanistic insights with a minimal computational expense.

Mechanistic Insights from Transition-State Theory

The unstable eigenmode from harmonic TST[5] and more generally the intrinsic reaction coordinate (IRC)[71–75] often provide excellent reaction coordinates for reactions that break and make strong chemical bonds.[32] Furthermore, the reaction path Hamiltonian,[76] constructed from the intrinsic arclength reaction coordinate s and minimum energy path in mass-weighted coordinates (MWC), can be used to understand the dynamics.[41] The potential energy surface in the reaction path Hamiltonian is a harmonic valley[76–80] around the minimum energy path. On a parabolic surface, mass weighted coordinates ($x_k = m_k^{1/2} q_k$ in the current study) transform the multidimensional equation "$F = ma$" into the simpler massless equation: $-\partial V/\partial \mathbf{x} = \mathrm{d}^2\mathbf{x}/\mathrm{d}t^2$. The multidimensional dynamics in mass-weighted coordinates can be simulated using Hamilton's equations from the reaction path Hamiltonian.[41,42]

The arclength coordinate in the (s, Q) subspace is sufficient to understand the role of Q in the reaction coordinate. Figure 7 shows the steepest-descent path, potential energy contours in the (s, Q) subspace, and the arclength coordinate as a colored background. Figure 7 also shows how the rate-promoting vibration frequency changes the role of Q in the arclength reaction coordinate. At very low frequencies, the reaction coordinate increases in the Q-direction, then increases in the s-direction, and finally increases again as Q decreases back to $Q = 0$. At higher frequencies of the RPV, s retains its primary importance in the reaction coordinate at early and late stages and at the transition state.

For $\omega_Q = 100$ cm^{-1}, the mass weighted arclength coordinate reveals three distinct stages of the reaction: (1) donor−acceptor approach [preorganization], (2) proton transfer at constant Q [instanton], and (3) donor−acceptor recede [reorganization]. In agreement with Antoniou et al.,[46] a low frequency ω_Q may allow several recrossings of the $s = 0$ surface, while the donor−acceptor pair are close. Portions of the reaction coordinate that involve Q also explain additional recrossing at multiples of $(2\pi/\omega_Q)$ after the initial crossing because of slow energy transfer from Q. Note that the three stages are no longer distinguishable at $\omega_Q = 900$ cm^{-1}.

TST cannot predict the extent or importance of dynamical effects, but harmonic TST actually reveals many of the mechanistic details in the RPV model. The Q values on the dividing surface from harmonic TST are markedly different from the values that characterize both the reactant and product states ($Q \approx 0$). For small ω_Q, the saddle-point ($Q = Q^*$) and the minima locations ($Q = 0$) and the real frequencies for displacement along Q (ω_Q in all three locations) reveal a situation at small ω_Q that is much like that in Figure 5b. Thus harmonic TST can identify a role for Q in pre- and re-organization.

For an actual enzyme, saddle-point search algorithms[70] would be needed to find the saddle point. The Hessian matrix at the saddle point could then be computed explicitly or numerically projected onto a few relevant bond lengths,[12] depending on the model chemistry. In the RPV model, the saddle point is trivially identified. The mass-weighted Hessian matrix at the saddle point is

$$\partial^2 V_{\mathrm{mwc}} = \begin{bmatrix} m_s^{-1}(\partial^2 V/\partial s^2)\big|_{\neq} & 0 & -m_s^{-1/2}\mathbf{c}^{\dagger}\mathbf{M}^{-1/2} \\ 0 & \omega_Q^2 & \mathbf{0} \\ -m_s^{-1/2}\mathbf{M}^{-1/2}\mathbf{c} & \mathbf{0} & \mathbf{\Omega}^2 \end{bmatrix} \tag{7}$$

where

$$\begin{aligned} \mathbf{M} &= \mathrm{diag}[m_1, m_2, \ldots, m_N] \\ \mathbf{\Omega} &= \mathrm{diag}[\omega_1, \omega_2, \ldots, \omega_N] \\ \mathbf{c}^{\dagger} &= (c_1, c_2, \ldots, c_N) \\ \left.\frac{\partial^2 V}{\partial s^2}\right|_{\neq} &= 2cQ^* - \frac{4V_0}{s_0^2} + \sum_k \frac{c_k^2}{m_k \omega_k^2} \end{aligned} \tag{8}$$

The unstable eigenmode *at the saddle point* has no contribution from the rate-promoting vibration. That is to be expected because of the symmetry of the potential energy surface. However, the unstable eigenmode is not perpendicular to the $s = 0$ plane. Bath modes influence the orientation of the unit normal vector on the dividing surface because of the off-diagonal coupling terms in the mass-weighted Hessian. To verify that the bath-mode contributions from harmonic TST do provide a more accurate reaction coordinate, we numerically diagonalized the mass-weighted Hessian for the exact parameters used by Antoniou and Schwartz.[53]

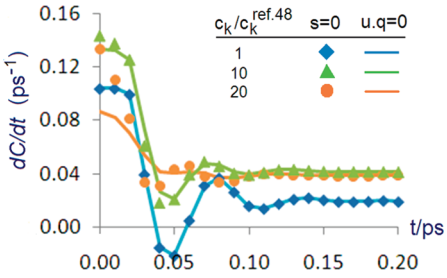

Figure 8. Reactive flux correlation function at different coupling strengths for the two dividing surfaces. The dividing surface $\mathbf{u}.\mathbf{q} = 0$ is always better than or equivalent to $s = 0$ in the variational sense. Parameters are those of Antoniou and Schwartz in ref 48.

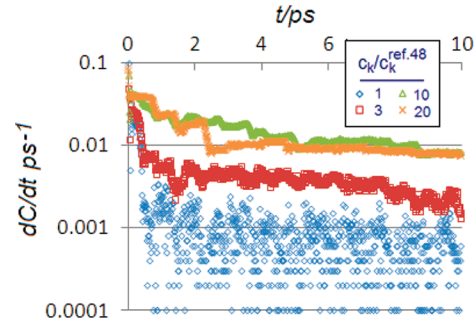

Figure 9. Using the dividing surface $\mathbf{u}.\mathbf{q} = 0$ in each case, dC/dt at longer times for four different coupling strengths. In Figure 8, dC/dt continues to decrease beyond the apparent plateau time. It is not clear whether a plateau in dC/dt can be identified. For the parameters of Antoniou and Schwartz, i.e., for c_k/c_k (ref 48) = 1, dC/dt rapidly decreases to a size where numerical errors exceed the physical value.

In their later work, Antoniou and Schwartz changed the barrier in $V_0(s)$ to 6.3 kcal/mol, ω_Q to 110 cm^{-1}, m_Q to 48 amu, all bath masses to $m_k = 48$ amu, and the transfer distance from 2 to 1 Å, i.e., $s_0 = 0.5$ instead of $s_0 = 1$ Å.[53] Antoniou and Schwartz also provided the bath frequencies used in their later study.[53] Again, the rate-promoting vibration Q was not directly coupled to a bath. Importantly, Antoniou and Schwartz used 10 times fewer bath modes (100 in the later study[53] vs 1000 in the earlier study)[46] with the same individual coupling strengths ($c_k = 0.00025$ au.) in both cases. The smaller bath results in significantly weaker coupling to the coordinate s. We used these parameters of Antoniou and Schwartz in a 200 ns trajectory. A time step of 0.04 fs was sufficiently small that the energy drift was less than 0.001kT over the entire 200 ns trajectory.

Transmission coefficients were computed using the hyperplane dividing surface perpendicular to the unstable eigenmode. Denoting the unstable eigenmode as $\mathbf{u}$ and denoting the mass-weighted position relative to the saddle point as $\mathbf{q}$, the dividing surface is $\mathbf{u}.\mathbf{q} = 0$, with positive values of $\mathbf{u}.\mathbf{q}$ indicating products. The transmission coefficient from the unstable eigenmode coordinate was compared to the transmission coefficient using $s = 0$ as the dividing surface. Figure 8 shows that at the coupling strength used by Antoniou and Schwartz, the $t = 0^+$ limit of dC/dt (and therefore the transmission coefficients) for $s = 0$ and $\mathbf{u}.\mathbf{q} = 0$ dividing surfaces are indistinguishable. However, as coupling increases the two surfaces become more different, with the unstable eigenmode giving the superior dividing surface. Thus harmonic TST can quantitatively validate the suggestion of Antoniou and Schwartz, who used subtle changes in distribution widths to argue that small components of the 'bath modes' may actually be part of an optimal reaction coordinate.[31,53,81,82]

Note that the plateau at ~0.2 ps is not a true plateau. At longer times, dC/dt continues to decrease, and it becomes difficult to identify a plateau. This behavior is shown for four coupling strengths in Figure 9. At the coupling strength used by Antoniou and Schwartz, dC/dt is becoming too small to accurately compute from the data in our simulations.[83] Interestingly, the value of dC/dt at times beyond 2 ps is approximately a linearly *increasing* function of coupling strength up to c_k/c_k (ref 48) = 10.[36] Then at c_k/c_k (ref 48) = 20, the value of dC/dt begins to decrease again, reminiscent of Kramers' turnover.[36] However, the apparent turnover occurs at coupling strengths that are an order of magnitude stronger than the coupling used by Antoniou and Schwartz.[53] Also note the appearance of discrete steps in dC/dt. The times between steps correspond approximately to $2\pi/\omega_Q$, a single orbit of the weakly coupled rate-promoting vibration. These observations all suggest that action angle variables for energy diffusion-limited kinetics in the promoting variable Q may provide good reaction coordinates in this system. However, we emphasize that energy diffusion limitations may entirely vanish for a real system with direct coupling between Q and the bath.

Conclusions

In the rate-promoting vibrations (RPV) model of enzyme catalysis, a 'promoting vibration' Q brings the donor and acceptor into proximity and lowers the barrier for motion along a 'proton-transfer coordinate' s. We studied dynamics in the RPV model using the parameters of Antoniou et al.[46] and also those of the later work by Antoniou and Schwartz.[53] The reactive flux correlation function for the RPV model shows that dynamical effects do slow the kinetics. However, the system shows an extremely narrow time scale separation because the parameters of Antoniou et al. give a barrier that is only 5kT high.[46] Additionally, we find strong correlations and surprising beats that persist in the dynamics of Q over times comparable to the reaction time scale. These unusual dynamical features result from a lack of direct coupling between Q and the bath in the RPV model. Near the reactant and product minima, Q also becomes effectively uncoupled from the proton-transfer coordinate s. Our findings suggest that direct coupling between Q and the bath may be needed to damp the beats and long-time correlations in the dynamics of Q.

Using the intrinsic reaction coordinate (IRC),[71–76] we show that Q is an important component of the reaction coordinate direction at early and late stages but not at the separatrix. Interestingly, the unstable eigenmode from harmonic TST (which coincides with the IRC at the saddle point) gives a larger transmission coefficient than the coordinate used in the correlation functions of Antoniou et al.[46,53] Additionally, harmonic TST is an important starting point for methods that

compute the energy landscape along the IRC to quantify effects of dynamics[41] and tunneling.[84] Our results thus support the view that promoting modes are a form of preorganization[8,21] and contrast the view that TST cannot provide insight on enzymatic reaction mechanisms.[45]

Finally, the relative merits and efficiencies of the procedure of Antoniou and Schwartz[53] for identifying reaction coordinates were compared to other approaches. We discuss how special 'promoting variables' can be identified by comparing the distribution of coordinate values in the reactant and product states and in the transition-state ensemble. Bath variables show a distribution of values in the transition-state ensemble that approximately interpolates between the reactant and product distributions. The distribution of promoting variable values in the transition-state ensemble will neither overlap nor interpolate between the distributions of promoting variable values in the reactant and product states. In agreement with Antoniou and Schwartz,[53] projecting the transition-state ensemble onto a good reaction coordinate should give a narrow distribution. However, their test only identifies the separatrix and thus is necessary but not sufficient to ensure an accurate reaction coordinate.[61]

Acknowledgment. I thank Gregg Beckham, Michael Hagan, and David Chandler for helpful discussions about this work. I acknowledge support from the Petroleum Research Fund of the American Chemical Society, PRF# 49165-DNI9.

References

(1) Pauling, L. *Nature* **1948**, *161*, 707.

(2) Radzicka, A.; Wolfenden, R. *Science* **1995**, *267*, 5194.

(3) Zhang, X. Y.; Houk, K. N. *Acc. Chem. Res.* **2005**, *38*, 379.

(4) Li, C. H.; Henry, C. S.; Jankowski, M. D.; Ionita, J. A.; Hatzimanikatis, V.; Broadbelt, L. J. *Chem. Eng. Sci.* **2004**, *59*, 5051.

(5) Hanggi, P.; Talkner, P.; Borkovec, M. *Rev. Mod. Phys.* **1990**, *62*, 251.

(6) Truhlar, D. G.; Garrett, B. C.; Klippenstein, S. J. *J. Phys. Chem.* **1996**, *100*, 12771.

(7) Garcia-Viloca, M.; Gao, J.; Karplus, M.; Truhlar, D. G. *Science* **2004**, *303*, 186.

(8) Warshel, A.; Sharma, P. K.; Kato, M.; Xiang, Y.; Liu, H.; Olsson, M. H. M. *Chem. Rev.* **2006**, *106*, 3188.

(9) Keck, J. *Adv. Chem. Phys.* **1967**, *13*, 85.

(10) Garrett, B. C.; Truhlar, D. G. *Annu. Rev. Phys. Chem.* **1984**, *35*, 159.

(11) Schenter, G. K.; Garrett, B. C.; Truhlar, D. G. *J. Chem. Phys.* **2003**, *119*, 5828.

(12) Rosta, E.; Woodcock, H. L.; Hummer, G.; Brooks, B. R. *J. Comput. Chem.* **2009**, *30*, 1634.

(13) Aqvist, J.; Warshel, A. *J. Am. Chem. Soc.* **1990**, *112*, 2860.

(14) Hu, H.; Yang, W. *Annu. Rev. Phys. Chem.* **2008**, *59*, 573.

(15) Warshel, A.; Levitt, M. *J. Mol. Biol.* **1976**, *103*, 227.

(16) Warshel, A. *J. Biol. Chem.* **1998**, *273*, 27035.

(17) Bruice, T. C.; Bruice, P. Y. *J. Am. Chem. Soc.* **2005**, *127*, 12478.

(18) Strajbl, M.; Sham, Y. Y.; Villa, J.; Chu, Z. T.; Warshel, A. *J. Phys. Chem. B* **2000**, *104*, 4578.

(19) Hammes-Schiffer, S.; Benkovic, S. *Annu. Rev. Biochem.* **2006**, *75*, 519.

(20) Hammes-Schiffer, S.; Tully, J. C. *J. Chem. Phys.* **1994**, *101*, 4657.

(21) Cui, Q.; Karplus, M. *J. Phys. Chem. B* **2002**, *106*, 7927.

(22) Senn, H. M.; Thiel, W. *Angew. Chem., Int. Ed.* **2008**, *48*, 1198.

(23) Gao, J. *Rev. Comput. Chem.* **1996**, *7*, 1996.

(24) Warshel, A.; Florian, J. *Empirical Valence Bond and Related Approaches*; Wiley and Sons: New York, NY, 2004.

(25) Agarwal, P. K.; Billeter, S. R.; Hammes-Schiffer, S. *J. Phys. Chem. B* **2002**, *106*, 3283.

(26) Benderskii, V. A.; Goldanskii, V. I.; Makarov, D. E. *Chem. Phys. Lett.* **1991**, *186*, 517.

(27) Billeter, S. R.; Webb, S. P.; Agarwal, P. K.; Iordanov, T.; Hammes-Schiffer, S. *J. Am. Chem. Soc.* **2001**, *123*, 11262.

(28) Pu, J.; Gao, J.; Truhlar, D. G. *Chem. Rev.* **2006**, *106*, 3140.

(29) Fernandez-Ramos, A.; Ellingson, B. A.; Garrett, B. C.; Truhlar, D. G. In *Reviews in Computational Chemistry*; Lipkowitz, K. B., Cundari, T. , Eds.; Wiley-VCH: Hoboken, NJ, 2007; Vol. 23.

(30) Dybala-Defratyka, A.; Paneth, P.; Banerjee, R.; Truhlar, D. G. *Proc. Nat. Acad. Sci. U.S.A.* **2007**, *104*, 10774.

(31) Truhlar, D. G.; Gao, J.; Garcia-Viloca, M.; Alhambra, C.; Corchado, J.; Sanchez, M. L.; Poulsen, T. D. *Int. J. Quantum Chem.* **2004**, *100*, 1136.

(32) Garcia-Viloca, M.; Truhlar, D. G.; Gao, J. *Biochemistry* **2003**, *42*, 13558.

(33) Rothlisberger, D.; Khersonsky, D.; Wollacot, A. M.; Jiang, L.; DeChancie, J.; Betker, J. L.; Gallaher, J. L.; Althoff, E. A.; Zanghellini, A.; Dym, O.; Albeck, S.; Houk, K. N.; Tawfik, D. S.; Baker, D. *Nature* **2008**, *453*, 190.

(34) Jiang, L.; Althoff, E. A.; Clemente, F. R.; Doyle, L.; Rothlisberger, D.; Zanghellini, A.; Gallaher, J. L.; Betker, J. L.; Tanaka, F.; Barbas, C. F.; Hilvert, D.; Houk, K. N.; Stoddard, B. L.; Baker, D. *Science* **2008**, *319*, 1387.

(35) Kuharski, R. A.; Chandler, D.; Montgomery, J. A.; Rabii, F.; Singer, S. J. *J. Phys. Chem.* **1988**, *92*, 3261.

(36) Kramers, H. A. *Physica* **1940**, *7*, 284.

(37) Chandler, D. *J. Chem. Phys.* **1978**, *68*, 2959.

(38) Straub, J. E.; Berne, B. *J. Chem. Phys.* **1985**, *83*, 1138.

(39) Vanden-Eijnden, E.; Tal, F. A. *J. Chem. Phys.* **2005**, *123*, 184103.

(40) Berne, B.; Borkovec, M.; Straub, J. E. *J. Phys. Chem.* **1988**, *92*, 3711.

(41) Peters, B.; Bell, A. T.; Chakraborty, A. K. *J. Chem. Phys.* **2004**, *121*, 4453.

(42) Hu, H.; Kobrak, M. N.; Xu, C.; Hammes-Schiffer, S. *J. Phys. Chem. A* **2000**, *104*, 8058.

(43) Hammes-Schiffer, S. *Biochemistry* **2002**, *41*, 13335.

(44) Kim, H. J.; Hynes, J. T. *J. Am. Chem. Soc.* **1992**, *114*, 10528.

(45) Pineda, J. R. E. T.; Schwartz, S. D. *Philos. Trans. R. Soc., B* **2006**, *361*, 1433.

(46) Antoniou, D.; Abolfath, M. R.; Schwartz, S. D. *J. Chem. Phys.* **2004**, *121*, 6442.

(47) Antoniou, D.; Basner, J.; Nunez, S.; Schwartz, S. D. *Chem. Rev.* **2006**, *106*, 3170.

(48) Quaytman, S.; Schwartz, S. D. *Proc. Nat. Acad. Sci. U.S.A.* **2007**, *104*, 12253.

(49) Schwartz, S. D.; Schramm, V. L. *Nat. Chem. Biol.* **2009**, *5*, 552.

(50) Bolhuis, P. G.; Dellago, C.; Chandler, D. *Faraday Discuss.* **1998**, *110*, 421.

(51) Dellago, C.; Bolhuis, P. G.; Chandler, D. *J. Chem. Phys.* **1998**, *108*, 9236.

(52) Bolhuis, P. G.; Chandler, D.; Dellago, C.; Geissler, P. G. *Annu. Rev. Phys. Chem.* **2002**, *53*, 291.

(53) Antoniou, D.; Schwartz, S. D. *J. Chem. Phys.* **2009**, *130*, 151103.

(54) Liu, F.; Nakaema, M.; Gruebele, M. *J. Chem. Phys.* **2009**, *131*, 195101.

(55) Caratzoulas, S.; Schwartz, S. D. *J. Chem. Phys.* **2001**, *114*, 2910.

(56) Best, R.; Hummer, G. *Proc. Nat. Acad. Sci. U.S.A.* **2005**, *102*, 6732.

(57) Ma, A.; Dinner, A. R. *J. Phys. Chem. B* **2005**, *109*, 6769.

(58) Peters, B.; Trout, B. L. *J. Chem. Phys.* **2006**, *125*, 054108.

(59) Peters, B.; Beckham, G. T.; Trout, B. L. *J. Chem. Phys.* **2007**, *127*, 1.

(60) Borrero, E. E.; Escobedo, F. A. *J. Chem. Phys.* **2007**, *127*, 164101.

(61) Peters, B. *J. Chem. Phys.* **2006**, *125*, 241101.

(62) Knott, B.; Duff, N. C.; Doherty, M. F.; Peters, B. *J. Chem. Phys.* **2009**, *131*, 224112.

(63) Peters, B.; Zimmerman, N. E. R.; Beckham, G. T.; Tester, J. W.; Trout, B. L. *J. Am. Chem. Soc.* **2008**, *130*, 17342.

(64) Juraszek, J.; Bolhuis, P. G. *Biophys. J.* **2008**, *95*, 4246.

(65) Beckham, G. T.; Peters, B.; Starbuck, C.; Variankaval, N.; Trout, B. L. *J. Am. Chem. Soc.* **2007**, *129*, 4714.

(66) Beckham, G. T.; Peters, B.; Trout, B. L. *J. Phys. Chem. B* **2008**, *112*, 7460.

(67) Vreede, J.; Juraszek, J.; Bolhuis, P. G. *Proc. Nat. Acad. Sci. U.S.A.* **2010**, *107*, 2397.

(68) Du, R.; Pande, V. S.; Grosberg, A. Y.; Tanaka, T.; Shakhnovich, E. S. *J. Chem. Phys.* **1998**, *108*, 334.

(69) Geissler, P. G.; Dellago, C.; Chandler, D. *J. Phys. Chem. B* **1999**, *103*, 3706.

(70) Schlegel, H. B. *J. Comput. Chem.* **2003**, *24*, 1514.

(71) Marcus, R. A. *J. Chem. Phys.* **1966**, *45*, 4500.

(72) Marcus, R. A. *J. Chem. Phys.* **1968**, *49*, 2610.

(73) Truhlar, D. G.; Kuppermann, A. *J. Am. Chem. Soc.* **1971**, *93*, 1840.

(74) Shavitt, I. *J. Chem. Phys.* **1968**, *49*, 4048.

(75) Fukui, K. *Acc. Chem. Res.* **1981**, *14*, 363.

(76) Miller, W. H.; Handy, N. C.; Adams, J. E. *J. Chem. Phys.* **1980**, *72*, 99.

(77) Garrett, B. C.; Truhlar, D. G. *J. Phys. Chem.* **1979**, *83*, 1052.

(78) Garrett, B. C.; Truhlar, D. G. *J. Phys. Chem.* **1979**, *83*, 1079.

(79) Garrett, B. C.; Truhlar, D. G. *Proc. Nat. Acad. Sci. U.S.A.* **1979**, *76*, 4755.

(80) Truhlar, D. G.; Garrett, B. C. *Acc. Chem. Res.* **1980**, *13*, 440.

(81) Truhlar, D. G.; Garrett, B. C. *J. Phys. Chem. B* **2000**, *104*, 1069.

(82) Pollak, E. *J. Chem. Phys.* **1986**, *85*, 865.

(83) Frenkel, D.; Smit, B. *Understanding molecular simulation: from algorithms to applications*; Academic Press: San Diego, CA, 2002.

(84) Peters, B.; Bell, A. T.; Chakraborty, A. K. *J. Chem. Phys.* **2004**, *121*, 4461.

CT100051A